RSC Advances

ROYAL SOCIETY OF CHEMISTRY

www.rsc.org/advances

RSC Advances

COMMUNICATION

Investigating the crystalline nature, charge transport properties and photovoltaic performances of ladder-type donor based small molecules

Received 00th January 20xx,
Accepted 00th January 20xx

DOI: 10.1039/x0xx00000x

www.rsc.org/

Hua-Chun Wang,[a]† Lu-Ming Tang,[a]† Lijian Zuo,[b] Hongzheng Chen*[b] and Yun-Xiang Xu*[a]

Four ladder-type donor based small molecules were synthesized and compared to investigate the influence of their core structures, π-bridge and end groups on the crytalline nature, charge transport and photovoltaic performances. The results showed that indacenodithieno[3,2-b]thiophene (IDTT) core was beneficial for the crytallinity and π-bridge structures could improve the photovoltaic performance.

Small molecule solar cells (OSCs) have been developed to be a competitive technique compared to their polymer counterparts, with reported power conversion efficiencies (PCEs) of above 10%,[1 2] possessing their unique advantages of monodispersity, high purity and batch-to-batch reproducibility.[3, 4] In terms of molecular design, many strategies have been adopted to improve the crystallinity, charge transport and phase separation of bulk-heterojunction blend films with fullerene derivatives, by tuning the structures of core motifs,[5] end groups, side chains and etc.[6, 7] Fused-ring units are usually incorporated into the backbone to ensure efficient intermolecular packing and thus continuous pathway of charge transport.[8] For planar fused-ring based structures, thanks to their semicrystalline nature, the structure-properties relationship have been clearly revealed. In contrast, fused rings with bulky side chains such as some ladder-type unit based molecules still lacked of a clear picture to depict the relationship among molecular structures, the corresponding nanomorphologies and properties, perhaps because the crystalline nature varied upon many factors in ladder-type unit based molecules.

It is well accepted that ladder-type fused rings have advantages in increasing the conjugation length and rigidity of according structures, which therefore enhance absorption ability and charge transport properties of according molecules.[9-11] Nevertheless, with the variations of bridge atoms, structures of side chains[6, 12] and backbones,[7, 13-16] modes of interchain interaction could be changed, as well as the nanomorphologies and charge transport properties. When alkyl side chains were adopted, some extent of ordering still exist in the scale of π-π stacking distance and lamellar distance, especially when the bridge atom is silicon.[5] However, when bulky side chains such as phenyl group were used, the steric hindered out-of-plane side chains will prohibit face-to-face packing of the aromatic backbones, usually resulting in noncrystalline materials.[17, 18] In this circumstance, π-π stacking very likely occurred at end groups, and the nature of end groups, such as dipoles,[19] planarity and rigidity become substantial to the final aggregation status and charge transport channels.

Indacenodithiophene (IDT)[20-24] and Indacenodithieno[3,2-b]thiophene (IDTT)[19] are two typical ladder-type moieties which were incorporated in various high performance electron donor or acceptor structures.[11, 25-31] For small molecules, usually amorphous or low-crystallinity materials were obtained after the π-bridge units and end groups were attached, which was thought to be intrinsic properties due to their out-of-plane side chains. However, during our study of IDTT-based small molecules, we found that IDTT itself actually possess high crystallinity and showed exceptional good hole mobility. Based on this observation, we designed a series of small molecules to investigate the relationship among molecules structures and crystallinity and charge transport properties. The results showed that not only the rigidity of the arm of molecules (including π-bridge units and end groups) but also the core structures affected the crystallinity. And the charge transport properties largely relied on the nature of arm structures. Their photovoltaic performances were also compared.

As shown in Scheme 1, four small molecules IDTT, IDTT-R, IDTT-T-T-R, and IDT-T-T-R were prepared and systematically compared. By attaching an electron withdrawing group

[a] College of Polymer Science & Engineering, State Key Laboratory of Polymer Materials Engineering, Sichuan University, Chengdu 610065, China. E-mail: yxxu@@scu.edu.cn
[b] State Key Laboratory of Silicon Materials, MOE Key Laboratory of Macromolecular Synthesis and Functionalization, Zhejiang University, Hangzhou, P. R. China. E-mail: hzchen@zju.edu.cn
† H.-C. W. and L.-M. T. contribute equally.
Electronic Supplementary Information (ESI) available: Supplementary information includes experimental section and characteristics data. See DOI: 10.1039/x0xx00000x

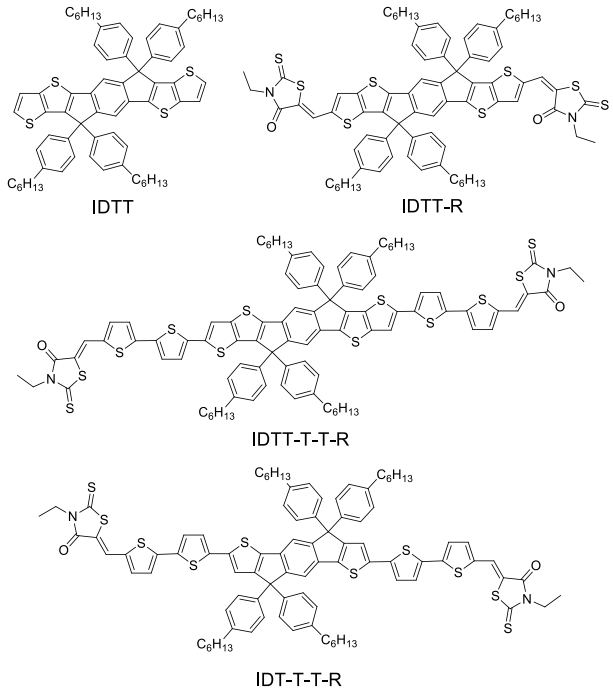

Scheme 1 Chemical structures of IDTT, IDTT-R, IDTT-T-T-R and IDT-T-T-R.

rhodanine on IDTT unit, IDTT-R become a donor-acceptor (D-A) structure with wider absorption range and lower LUMO level. IDTT-T-T-R and IDT-T-T-R have two more thiophene π-bridge units, but different core structures. The detailed synthesis route and purification procedures were included in supporting information. It is worthy noticed that all the molecules can be readily dissolved in chlorinated solvents, such as chloroform and dichlorobenzene (DCB), except for IDTT-T-T-R which is only barely soluble in DCB.

Thermal analysis was first utilized to probe the crystalline nature of these compounds by differential scanning calorimetry (DSC) measurement at a temperature ramp rate of 10 °C/min under nitrogen（Figure S1). It is shown that IDTT exhibited sharp thermal transitions during the heating/cooling cycle, indicating a reversible crystal-crystal transition. However, when end group was attached for IDTT-R, the transition peaks became broad, with a melting endothermic peak around 175 °C on heating and two exothermic transition upon cooling, which implies its conformational polymorphs. With bithiophene π-bridge units attached, IDTT-T-T-R showed peaks only in heating curve. And for IDT-T-T-R, the thermal transition is weakest and irreversible. The trend demonstrated by these four compounds indicated that the crystallinity become weaker with the arm structures becoming longer. And the extended core structure of IDTT is more beneficial for the crystallization compared with IDT core.

Then the X-ray diffraction (XRD) experiments were performed to reveal the molecular ordering of these compounds. Consistent with the above DSC experimental results, IDTT exhibited distinct diffraction signals. The peak at

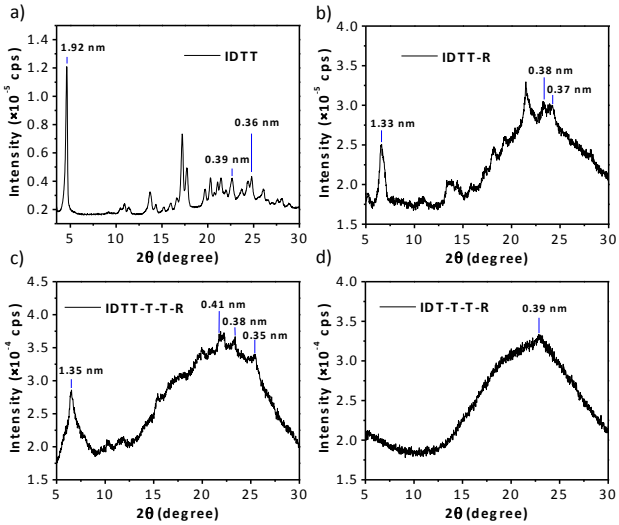

Fig. 1 XRD curves of a) IDTT; b) IDTT-R; c) IDTT-T-T-R and d) IDT-T-R.

1.92 nm (2θ = 4.64°) indicated typical lamellar spacing while the peaks between 3.5 Å to 4.0 Å demonstrated strong π-π stacking. Since the single crystal of IDTT was not obtained, it is difficult to identify every peak. For IDTT-R and IDTT-T-T-R, the π-π stacking peaks were much broader than IDTT and lamellar peaks still existed at around 1.33 nm (2θ = 6.61°) and 1.35 nm (2θ = 6.56°), suggesting that their aromatic packing become more disordered, but with some extent of lamellar ordering. It is noticed that IDTT-R exhibited a little sharper peaks than IDTT-T-T-R, maybe due to its shorter and more rigid arm structure. Considering the structural difference of IDTT, IDTT-R and IDTT-T-T-R, it is rational to conclude that introducing arm structures will weaken the ordering of π-π stacking, perhaps due to the diminished rigidity of whole backbone when more units were attached. While the core structure was altered from IDTT to IDT, the compound IDT-T-T-R didn't show any obvious peak, indicating its amorphous nature. Therefore extended fused ring IDTT was beneficial for the molecular ordering, probably by increasing the rigidity of molecules.

Intimately relating to the film crystalline properties, the charge transporting behaviors were expected to be different with altered core structure, arm length, and end groups. To investigate the intrinsic charge transport properties of these compounds, bottom gate and top-contact organic field-effect transistors (OFET) were fabricated. The corresponding parameters are shown in Table 1 except for IDTT-T-T-R which failed to get qualified films due to its poor solubility. As shown in the Table 1, IDTT films prepared from chloroform (CF) and dichlorobenzene (DCB) solution showed hole mobilities of 4.2×10^{-2} $cm^2V^{-1}s^{-1}$ and 1.3×10^{-2} $cm^2V^{-1}s^{-1}$ respectively, which are decent for ladder-type donor based molecules. In contrast, for IDTT-R and IDT-T-T-R, the films prepared from DCB solution have much lower hole mobilities of 8.1×10^{-7} and 3.69×10^{-5} $cm^2V^{-1}s^{-1}$, respectively. However, compared with IDTT and IDT-T-T-R, IDTT-R possesses the best electron mobility of 5.4×10^{-3} $cm^2V^{-1}s^{-}$

Table 1 FET characteristics of IDTT, IDTT-R and IDT-T-T-R.

Small molecule	Hole Mobility ($cm^2 V^{-1} s^{-1}$)	On/Off Ratio	V_t (V)	Electron Mobility ($cm^2 V^{-1} s^{-1}$)	On/Off Ratio	V_t (V)
IDTT (DCB)	1.3E-2	8.4E+5	-29	4.4E-6	6.6E+5	30
IDTT (CF)	4.2E-2	2E+6	-5	2.9E-8	1.7E+7	56
IDTT-R (DCB)	8.1E-7	1.8E+4	-44	5.4E-3	8.6E+3	26
IDT-T-T-R (DCB)	3.69E-5	2.8E+4	-41	4.8E-4	1.1E+4	25

[1], which remind us of the recently reported nonfullerene acceptors based on IDT and IDTT moieties.[25-27] Since the charge transport not only relied on the reorganization energies each molecule possessed, but also the molecular orbital overlaps in the solid states, which can be influenced by the rigidity of the backbones, and the stacking mode of the arm structures. In our case, it is not clear about the mode of intermolecular interactions, but for the rigidity of backbones we can get some clues from the observations in the XRD and DSC experiments. IDTT based molecules with shorter arm structures seems possess more rigid backbones, which showed higher extent of crystallinity, and also demonstrated either higher hole mobility (for IDTT) or electron mobility (for IDTT-R). Thus it is reasonable to suggest that even better hole or electron mobility could be approached by controlling the rigidity of molecules and choosing the arm structures cautiously.

To get the information about their absorption ability and molecular orbital energy levels, UV–vis absorption spectra and cyclic voltammetry (CV) curves were acquired. The normalized solution and thin film UV–vis spectra of all four compounds are displayed in Figure 2 and some important optical parameters are summarized in Table S1. In dilute dichlorobenzene (DCB) solution, the absorption of IDTT-R was red-shifted 159 nm compared with that of IDTT, due to the formation of D-A structures. When π-bridge was introduced, the absorption peaks of IDTT-T-T-R and IDT-T-T-R became broader because of the extended conjugation length. However, their maximum peaks blue-shifted compared with IDTT-R, probably due to the reduced intramolecular charge transfer. All maximum peaks of films of IDTT-based compounds red-shifted about 16-17 nm compared with their solution peaks, which maybe stemmed

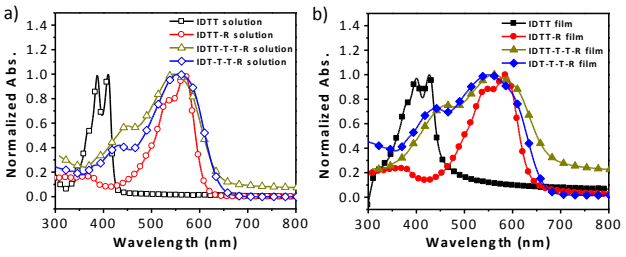

Fig. 2 Normalized UV–Vis absorption spectra of IDTT, IDTT-R, IDTT-T-T-R and IDT-T-T-R a) in DCB solution; b) in films.

from efficient intermolecular π-π stacking between arm structures. Nevertheless, for IDT-T-T-R, a hypsochromic absorption peak at 550 nm in its solid state was observed compared with 554 nm in its solution state, which was usually attributed to the twist of its backbone. This phenomena is consistent with the assumption that IDTT unit could increase the rigidity of molecular backbone, while IDT unit not. CV measurement (Figure S2) showed close HOMO and LUMO values for IDTT-R, IDTT-T-T-R and IDT-T-T-R, with LUMO levels around -3.50 eV, which should be high enough to drive the exciton dissociation in blend with fullerenes.

To evaluate photovoltaic properties of BHJ solar cells using IDTT-R, IDTT-T-T-R and IDT-T-T-R as donor materials, devices are fabricated with the configuration ITO/PEDOT:PSS/donor:$PC_{71}BM$ (1:2)/Bis-C_{60} /Ag.[32] The detailed device fabrication procedure is described in the Supporting Information. The current density–voltage (J–V) curves for devices are measured under simulated AM1.5G illumination at 100 mW cm^{-2} and shown in Figure 3a. The performance of these devices is summarized in Table 2. IDTT-R derived devices performed very poor although the absorption of which is close to IDTT-T-T-R and IDT-T-T-R, which could be mainly attributed to the limited end groups interactions failing to promote a proper phase separation, especially considering the obtained much lower open-circuit voltage (V_{oc}). For IDTT-T-T-R and IDT-T-T-R, their large arm structures could increase the intermolecular interactions and help the formation of better phase separation. As mentioned before, the IDTT-T-T-R compound has limited solubility in DCB, which may affect the optimization of nanomorphologies. Indeed, according to the surface nanomorphologies revealed by atomic force microscopy (AFM) experiments, the root-mean-square (RMS) surface roughness of IDTT-T-T-R blend films (86 nm, Figure S3) is much larger than those of IDTT-R (0.36 nm)

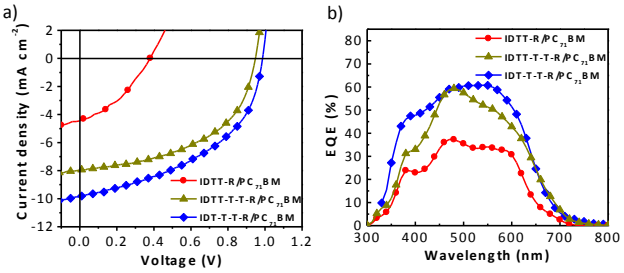

Fig. 3 a) Characteristic J–V curves and b) EQE for the BHJ solar cells derived from IDTT-R, IDTT-T-T-R and IDT-T-T-R.

Table 2 Device performance parameters for BHJ solar cells based on IDTT-R, IDTT-T-T-R and IDT-T-T-R.

Device	J_{sc} (mA cm^{-2})	V_{oc} (V)	*FF* (%)	PCE (%)
IDTT-R/$PC_{71}BM$	4.38	0.50	35	0.77
IDTT-T-T-R/$PC_{71}BM$	7.99	0.95	51	3.86
IDT-T-T-R/$PC_{71}BM$	9.83	0.99	47	4.56

and IDT-T-T-R (0.48 nm), and heavily aggregated domains (above 100 nm) were also observed for IDTT-T-T-R blend films.[33] These oversized domains may affect the efficiency of exciton dissociation, which could account for the inferior short-circuit current density (J_{sc}) value of IDTT-T-T-R device (7.99 mA cm^{-2}) relative to that of IDT-T-T-R (9.83 mA cm^{-2}). Finally, the device based on IDT-T-T-R got the highest PCE of 4.56% with a V_{oc} of 0.99 V, a J_{sc} of 9.83 mA cm^{-2}, and a fill factor (*FF*) of 0.47. While the IDTT-T-T-R device showed a lower PCE of 3.86% with a V_{oc} of 0.95 V, a J_{sc} of 7.99 mA cm^{-2}, and an *FF* of 0.51. The external quantum efficiency (EQE) is measured to verify the performance of the above devices. As shown in Figure 3b, the EQE curves of IDTT-R, IDT-T-T-R and IDTT-T-T-R exhibit broad responses from 330 to 700 nm. The calculated J_{sc} values by integration of the EQE curves match well with those obtained from the J–V measurements.

In conclusion, three IDTT-based small molecules and one IDT-based molecule were prepared and systematically compared, to investigate the influence of core structures and arm structures on their crystalline nature, charge transport and photovoltaic performances. The results showed that IDTT as a core unit could increase the crystallinity of compounds. However, with longer arms the crystallinity is weaker, perhaps due to the reduced rigidity of whole backbones. The charge transport properties and photovoltaic performances depend on the solid states derived from these compounds. The large arm structures should enhanced intermolecular interactions which is beneficial for the continuous phase formation. However, the way the molecules packed and their detailed nanomorphologies need to be explored further.

Acknowledgements

We thank the financial support from the National Natural Science Foundation of China (51403135) and State Key Laboratory of Polymer Materials Engineering (Grant No. sklpme2014-3-16).

References

1. B. Kan, M. Li, Q. Zhang, F. Liu, X. Wan, Y. Wang, W. Ni, G. Long, X. Yang, H. Feng, Y. Zuo, M. Zhang, F. Huang, Y. Cao, T. P. Russell and Y. Chen, *J. Am. Chem. Soc.*, 2015, **137**, 3886-3893.
2. B. Kan, Q. Zhang, M. Li, X. Wan, W. Ni, G. Long, Y. Wang, X. Yang, H. Feng and Y. Chen, *J. Am. Chem. Soc.*, 2014, **136**, 15529-15532.
3. K. Sun, Z. Xiao, S. Lu, W. Zajaczkowski, W. Pisula, E. Hanssen, J. M. White, R. M. Williamson, J. Subbiah, J. Ouyang, A. B. Holmes, W. W. H. Wong and D. J. Jones, *Nat. Commun.*, 2015, **6**, doi:10.1038/ncomms7013.
4. Q. Zhang, B. Kan, F. Liu, G. Long, X. Wan, X. Chen, Y. Zuo, W. Ni, H. Zhang, M. Li, Z. Hu, F. Huang, Y. Cao, Z. Liang, M. Zhang, T. P. Russell and Y. Chen, *Nat. Photon.*, 2015, **9**, 35-41.
5. J. A. Love, I. Nagao, Y. Huang, M. Kuik, V. Gupta, C. J. Takacs, J. E. Coughlin, L. Qi, T. S. van der Poll, E. J. Kramer, A. J. Heeger, T.-Q. Nguyen and G. C. Bazan, *J. Am. Chem. Soc.*, 2014, **136**, 3597-3606.
6. X. Liu, Q. Li, Y. Li, X. Gong, S.-J. Su and Y. Cao, *J. Mater. Chem. A*, 2014, **2**, 4004-4013.
7. J.-L. Wang, Q.-R. Yin, J.-S. Miao, Z. Wu, Z.-F. Chang, Y. Cao, R.-B. Zhang, J.-Y. Wang, H.-B. Wu and Y. Cao, *Adv. Funct. Mater.*, 2015, **25**, 3514-3523.
8. L. Yuan, Y. Zhao, J. Zhang, Y. Zhang, L. Zhu, K. Lu, W. Yan and Z. Wei, *Adv. Mater.*, 2015, **27**, 4229-4233.
9. R. Noriega, J. Rivnay, K. Vandewal, F. P. V. Koch, N. Stingelin, P. Smith, M. F. Toney and A. Salleo, *Nat. Mater.*, 2013, **12**, 1038-1044.
10. X. Zhang, H. Bronstein, A. J. Kronemeijer, J. Smith, Y. Kim, R. J. Kline, L. J. Richter, T. D. Anthopoulos, H. Sirringhaus, K. Song, M. Heeney, W. Zhang, I. McCulloch and D. M. DeLongchamp, *Nat. Commun.*, 2013, **4**, 2238.
11. Y.-X. Xu, C.-C. Chueh, H.-L. Yip, F.-Z. Ding, Y.-X. Li, C.-Z. Li, X. Li, W.-C. Chen and A. K. Y. Jen, *Adv. Mater.*, 2012, **24**, 6356-6361.
12. Q. Zheng, S. Chen, B. Zhang, L. Wang, C. Tang and H. E. Katz, *Org. Lett.*, 2011, **13**, 324-327.
13. J.-L. Wang, Z. Wu, J.-S. Miao, K.-K. Liu, Z.-F. Chang, R.-B. Zhang, H.-B. Wu and Y. Cao, *Chem. Mater.*, 2015, **27**, 4338-4348.
14. Y. Ma, Q. Zheng, L. Wang, D. Cai, C. Tang, M. Wang, Z. Yin and S.-C. Chen, *J. Mater. Chem. A*, 2014, **2**, 13905-13915.
15. L. Wang, D. Cai, Z. Yin, C. Tang, S.-C. Chen and Q. Zheng, *Polym. Chem.*, 2014, **5**, 6847-6856.
16. Y. Ma, Q. Zheng, Z. Yin, D. Cai, S.-C. Chen and C. Tang, *Macromolecules*, 2013, **46**, 4813-4821.
17. J. H. Kim, J. W. Jung, S. T. Williams, F. Liu, T. P. Russell and A K. Y. Jen, *Nanoscale*, 2015, **7**, 10936-10939.
18. K. Yao, Y.-X. Xu, F. Li, X. Wang and L. Zhou, *Adv. Opt. Mater.*, 2015, **3**, 321-327.
19. J. J. Intemann, K. Yao, F. Ding, Y. Xu, X. Xin, X. Li and A. K. Y. Jen, *Adv. Funct. Mater.*, 2015, DOI: 10.1002/adfm.201501600.
20. D. Liu, M. Xiao, Z. Du, Y. Yan, L. Han, V. A. L. Roy, M. Sun, W. Zhu, C. S. Lee and R. Yang, *J. Mater. Chem. C*, 2014, **2**, 7523-7530.
21. H. Bai, Y. Wang, P. Cheng, Y. Li, D. Zhu and X. Zhan, *ACS Appl. Mater. Interfaces*, 2014, **6**, 8426-8433.
22. W. Tang, D. Huang, C. He, Y. Yi, J. Zhang, C. Di, Z. Zhang and Y. Li, *Org. Electron.*, 2014, **15**, 1155-1165.
23. H. Bai, P. Cheng, Y. Wang, L. Ma, Y. Li, D. Zhu and X. Zhan, *J. Mater. Chem. A*, 2014, **2**, 778-784.
24. W. Yong, M. Zhang, X. Xin, Z. Li, Y. Wu, X. Guo, Z. Yang and J Hou, *J. Mater. Chem. A*, 2013, **1**, 14214-14220.
25. H. Bai, Y. Wang, P. Cheng, J. Wang, Y. Wu, J. Hou and X. Zhan, *J. Mater. Chem. A*, 2015, **3**, 1910-1914.
26. Y. Lin, J. Wang, Z.-G. Zhang, H. Bai, Y. Li, D. Zhu and X. Zhan, *Adv. Mater.*, 2015, **27**, 1170–1174.
27. Y. Lin, Z.-G. Zhang, H. Bai, J. Wang, Y. Yao, Y. Li, D. Zhu and X Zhan, *Energy Environ. Sci.*, 2015, **8**, 610-616.

28. X. Xu, Z. Li, O. Backe, K. Bini, D. I. James, E. Olsson, M. R. Andersson and E. Wang, *J. Mater. Chem. A*, 2014, **2**, 18988-18997.
29. J. J. Intemann, K. Yao, Y.-X. Li, H.-L. Yip, Y.-X. Xu, P.-W. Liang, C.-C. Chueh, F.-Z. Ding, X. Yang, X. Li, Y. Chen and A. K. Y. Jen, *Adv. Funct. Mater.*, 2014, **24**, 1465–1473.
30. Y.-x. Xu, C.-C. Chueh, H.-L. Yip, C.-Y. Chang, P.-W. Liang, J. Intemann, W.-C. Chen and A. Jen, *Polym. Chem.*, 2013, **4**, 5220-5223.
31. Y. Zang, Y.-X. Xu, C.-C. Chueh, C.-Z. Li, H.-C. Chen, K.-H. Wei, J.-S. Yu and A. K. Y. Jen, *RSC Adv.*, 2015, **5**, 26680-26685.
32. K. M. O'Malley, C.-Z. Li, H.-L. Yip and A. K. Y. Jen, *Adv. Energy Mater.*, 2012, **2**, 82-86.
33. J. Wang, M. Xiao, W. Chen, M. Qiu, Z. Du, W. Zhu, S. Wen, N. Wang and R. Yang, *Macromolecules*, 2014, **47**, 7823-7830.